J. Plasma Physics (2012), vol. 78, part 4, pp. 447–453. © Cambridge University Press 2012
doi:10.1017/S0022377812000311

Laser plasma accelerator driven by a super-Gaussian pulse

TOBIAS OSTERMAYR[1], STEFAN PETROVICS[1], KHALID IQBAL[1], CONSTANTIN KLIER[1], HARTMUT RUHL[1], KAZUHISA NAKAJIMA[3,4,5], AIHUA DENG[3], XIAOMEI ZHANG[3], BAIFEI SHEN[3], JIANSHENG LIU[3], RUXIN LI[3], ZHIZHAN XU[3] and TOSHIKI TAJIMA[1,2]

[1]Ludwig-Maximilians-Universität München, 85748 Garching, Germany
(tobias.ostermayr@physik.uni-muenchen.de)
[2]Max-Planck-Institut für Quantenoptik, Garching 85748, Germany
[3]Shanghai Institute of Optics and Fine Mechanics, Chinese Academy of Sciences, Shanghai 201800, China
[4]High Energy Accelerator Research Organization, 1-1 Oho, Tsukuba, Ibaraki 305-0081, Japan
[5]Shanghai Jiao Tong University, Shanghai 200240, China

(Received 30 September 2011; revised 24 January 2012; accepted 7 March 2012; first published online 12 April 2012)

Abstract. A laser wakefield accelerator (LWFA) with a weak focusing force is considered to seek improved beam quality in LWFA. We employ super-Gaussian laser pulses to generate the wakefield and study the behavior of the electron beam dynamics and synchrotron radiation arising from the transverse betatron oscillations through analysis and computation. We note that the super-Gaussian wakefields radically reduce the betatron oscillations and make the electron orbits mainly ballistic over a single stage. This feature permits to obtain small emittance and thus high luminosity, while still benefitting from the low-density operation of LWFA (Nakajima et al. 2011 *Phys. Rev. ST Accel. Beams* **14**, 091301), such as the reduced radiation loss, less number of stages, less beam instabilities, and less required wall plug power than in higher density regimes.

1. Introduction

During the past few decades after the first suggestion of a laser plasma accelerator by Tajima and Dawson (1979), thanks to vital research, the development of laser-driven plasma accelerators (LPAs) has achieved major results. After the first proof-of-principle experiments (Modena et al., 1995; Nakajima et al., 1995), LPA experiments also demonstrated the production of electron beams with energies in the GeV regime (Leemans et al., 2006; Clayton et al., 2010), with high quality of energy spread (1% level) (Kameshima et al., 2008) and transverse emittance (1-πmm-mrad level) (Karsch et al., 2007) in addition to 1-fs level bunch duration (Lundh et al., 2011). These characteristics ensure the high stability of reproduction, which is on par with present high-power ultrashort-pulse lasers with controlled injection (Hafz et al., 2008; Osterhoff et al., 2008). Today it is a very promising technology for compact next generation accelerators with a broad range of applications such as radiolysis (Crowell et al., 2004; Brozek-Pluskab et al., 2005), electron diffraction (van Outheusden et al., 2010), intraoperative radio therapy (Giulietti et al., 2008), radiation sources of terahertz (THz) (Hamster et al., 1993; Leemans et al., 2003), and others. In particular, the scale and cost of large-scale particle accelerators, such as high-energy colliders, could be reduced. Most of the above-cited experimental results were conducted using ultrashort ($\sim 30-80$ fs) laser pulses interacting with short plasmas, such as gas jets with lengths ranging from few millimeters to few centimeters with plasma densities of $10^{18}-10^{19}$ cm^{-3}. There the acceleration of electrons to energies of the order of 1 GeV is accomplished by the efficient trapping of electrons in the wake with an accelerating gradient of the order of 100 GeVm^{-1}.

The leading experiments demonstrating the production of quasi-monoenergetic electron beams (Faure et al., 2004; Geddess et al., 2004; Mangles et al., 2004) used self-injection and subsequent acceleration of electrons in a nonlinear wakefield, the so-called bubble (Kostyukov et al., 2004; Lu et al., 2006), which is characterized by its normalized vector potential, $a_0 = \varepsilon A_0/m_e c^2 \gg 1$, where A_0 is the peak amplitude of the vector potential and m_e is the rest mass of the electron. The bubble is a region where plasma electrons are blown out due to radiation pressure of a laser pulse with relativistic intensity. Self-injection occurs due to self-focusing and self-compression if the drive laser exceeds the threshold power, $(P/P_c)_{th} \approx 3$ (Froula et al., 2009), where $P_c \approx 17(\omega_0/\omega_p)^2$ GW is the critical power for the relativistic self-focusing with laser frequency ω_0 and plasma frequency $\omega_p = \sqrt{4\pi e^2 n_e/m_e}$. The suppression of self-injection and betatron oscillations is important to produce high-quality beams, as they are required for most of the possible applications. Several experiments were carried out using controlled injection mechanisms such as colliding optical injection (Faure et al., 2006), density-transition injection (Schmid et al.,

2010), ionization-induced injection (McGuffey et al., 2010; Pak et al., 2010), and two-stage laser plasma accelerator with ionization-induced injection (Liu et al., 2011; Pollock et al., 2011) in the quasi-linear regime, which is characterized by a moderate intensity of the drive laser pulse of $a_0 \sim 1$, providing high-quality GeV-class electron beam injectors.

High-energy accelerator applications of LPA require a multistage setup to achieve the desired energy gain for electrons, since the acceleration length of a single LPA stage is limited by dephasing length and/or by the energy-depletion length of the drive laser pulse. Minimizing the total linac length for an LPA with final beam energy of 0.5 TeV, a drive laser intensity of $a_0 = 1.5$, and a coupling distance of $\leqslant 1$ m leads to the operating plasma density of $n_e = 10^{17}$ cm^{-3} (Schroeder et al., 2010). In this density regime, several possible designs of LPA linac colliders have been conceived (Tajima, 1985; Xie et al., 1997; Schroeder et al., 2010). Recent considerations (Nakajima et al., 2011) took into account further constraints on the plasma density. For example, further considerations on the coupling section installing both laser and beam focusing systems, which realistically might require a distance of the order of several meters using conventional technologies, instead of that previously considered less than 1 m, leading to a reduced optimum operating plasma density of $10^{15}-10^{16}$ cm^{-3} rather than 10^{17} cm^{-3}. In addition, the technology allowing to preform a large-scale plasma channel also points plasma density to the same region of $10^{15}-10^{16}$ cm^{-3}. It was shown (Nakajima et al., 2011) that the low-density regime with $n_e = 10^{15}$ cm^{-3} has a number of advantages, such as the reduced radiation loss, the reduced number of stages, the reduced beam instabilities, and significantly the reduced wall plug power, while the lower density requires a very large laser peak power of ~ 11 PW and a laser energy of ~ 10 kJ per pulse for a stage of 0.5 TeV. These requirements on the laser have not been matched by any existing laser system so far. It was also pointed out that a large number of stages, as required in higher density regimes, such as $n_e \sim 10^{17}$ cm^{-3}, makes the low emittance beam dynamics very challenging (Cheshkov et al., 2000; Chiu et al., 2000). Generally, the operation at low-plasma density increases the single-stage energy gain and the pump depletion length L_{pd}, while it reduces the accelerating gradient and the number of stages.

Application of multi-staged LPAs in the field of high-energy physics requires extreme high-quality beams with small energy spread and transverse emittance as well as sufficiently large charge/number of particles per bunch. We find that besides the advantages of a low-density LPA linac design, there is one problem arising from simultaneous requirements on both the transverse emittance as well as the particle number per bunch. We focus on this problem in this paper. In order to preserve the loaded charge of the accelerated particle beam $Q_b \sim \sigma_{x0}^2\sqrt{n_e}$ while decreasing the density, the initial radius of the particle beam σ_{x0} needs to be increased. And since $\sigma_{x0}^2 \sim \varepsilon_{n0}$, this leads to an increased initial emittance ε_{n0} of the particle beam. Nakajima et al. (2011) showed that radiation damping is not sufficient to cool the beam down to a reasonable value of emittance during acceleration for the range of TeV in low-density regime.

In this paper we employ laser pulses with a super-Gaussian radial profile to drive the laser wakefield. This technology allows for a small initial emittance while keeping the radius of the beam large enough to fulfill the requirements for a large number of particles and therefore sufficient luminosity. We will show that the super-Gaussian wakefield reduces the betatron oscillations radically and makes the electron orbits mainly ballistic over a single stage of acceleration while keeping the emittance at an almost constant level. The formulas utilized for tailoring a super-Gaussian wakefield are presented in Sec. 2. Considering beam dynamics, analytical estimates for betatron oscillation and radiation damping in different cases of super-Gaussian pulse-driven wakefields are evaluated in Sec. 3. Based on our results, in Sec. 4 we deliberate on possible future steps toward experimental realizations of super-Gaussian laser pulses for tailoring a laser wakefield.

2. Laser wakefield with super-Gaussian laser pulse

In this paper we study the quasi-linear laser wakefield regime characterized by the normalized peak intensity of linearly polarized laser pulse $a_0 = 0.85(I\lambda^2/10^{18}\ \mathrm{Wcm^{-2}\mu m^2})^{1/2} \sim 1$, where I is the laser peak intensity and $\lambda = 2\pi c/\omega_0$ is the laser wavelength. The wake potential Φ is obtained from a simple harmonic equation (Gorbunov and Kirsanov, 1987; Sprangle et al., 1988),

$$\frac{\partial^2\Phi}{\partial\zeta^2} + k_p^2\Phi = k_p^2 m_e c^2 \frac{a^2(r,\zeta)}{2}, \tag{2.1}$$

where $\zeta = z - v_g t$ and $v_g = c\sqrt{(1-\omega_p^2/\omega_0^2)}$ is the group velocity of the laser pulse, $a^2(r,\zeta)$ is defined in (2.4), and $k_p = \omega_p/c$ is the plasma wave number. The wake potential Φ is calculated as

$$\Phi(r,\zeta) = -\frac{m_e c^2 k_p}{2}\int_\zeta^\infty \mathrm{d}\zeta' \sin k_p(\zeta-\zeta')a^2(r,\zeta'). \tag{2.2}$$

The axial and radial electric fields are given by

$$eE_z = -\frac{\partial\Phi}{\partial z} \quad \text{and} \quad eE_r = -\frac{\partial\Phi}{\partial r}. \tag{2.3}$$

Consider a temporally Gaussian laser pulse, of which the ponderomotive potential is given by

$$a^2(r,\zeta) = U(r)\exp\left(-\frac{\zeta^2}{\sigma_z^2}\right). \tag{2.4}$$

The coefficient $U(r)$ is considered below. The wake potential may be calculated as

$$\Phi(r,\zeta) = -BU(r)[C(\zeta)\sin k_p\zeta + S(\zeta)\cos k_p\zeta], \tag{2.5}$$

https://doi.org/10.1017/S0022377812000311 Published online by Cambridge University Press

where

$$B = \frac{\sqrt{\pi} m_e c^2 k_p \sigma_z}{4} \exp\left(-\frac{k_p^2 \sigma_z^2}{4}\right), \tag{2.6}$$

$$C(\zeta) = 1 - \mathrm{Re}\left[\mathrm{erf}\left(\frac{\zeta}{\sigma_z} - i\frac{k_p \sigma_z}{2}\right)\right], \tag{2.7}$$

$$S(\zeta) = \mathrm{Im}\left[\mathrm{erf}\left(\frac{\zeta}{\sigma_z} - i\frac{k_p \sigma_z}{2}\right)\right], \tag{2.8}$$

and $\mathrm{erf}(z) = \frac{2}{\sqrt{\pi}} \int_0^z e^{-z'^2} \mathrm{d}z'$ is the error function. This leads to the axial and radial electric fields

$$eE_z(r,\zeta) = -\frac{\partial \Phi}{\partial \zeta} = Bk_p U(r)[C(\zeta)\cos k_p\zeta - S(\zeta)\sin k_p\zeta], \tag{2.9}$$

$$eE_r(r,\zeta) = -\frac{\partial \Phi}{\partial r} = B\frac{\partial U(r)}{\partial r}[C(\zeta)\sin k_p\zeta + S(\zeta)\cos k_p\zeta]. \tag{2.10}$$

Behind the laser pulse, $\zeta \ll \sigma_z$, $C(\zeta) \to 2$ and $S(\zeta) \to 0$. The wakefields are then given by

$$eE_z(r,\zeta) = 2Bk_p U(r)\cos k_p\zeta, \tag{2.11}$$

$$eE_r(r,\zeta) = 2B\frac{\partial U(r)}{\partial r}\sin k_p\zeta. \tag{2.12}$$

We now investigate wakefields created by radially super-Gaussian laser fields. The radial potential profile is described by super-Gaussian functions

$$U(r) = a_0^2 \exp\left(-\frac{2r^n}{r_L^n}\right), \tag{2.13}$$

where $n \geqslant 2$. In this paper n denotes the power of the super-Gaussian potential. A Gaussian profile corresponds to $n = 2$. For a super-Gaussian potential, the axial and radial wakefields are derived as

$$eE_z(r,\zeta) = \frac{\sqrt{\pi}}{2} a_0^2 m_e c^2 k_p^2 \sigma_z \exp\left(-\frac{2r^n}{r_L^n} - \frac{k_p^2\sigma_z^2}{4}\right) \times \cos k_p\zeta, \tag{2.14}$$

$$eE_r(r,\zeta) = -n\sqrt{\pi} a_0^2 m_e c^2 k_p \sigma_z \frac{r^{n-1}}{r_L^n} \exp\left(-\frac{2r^n}{r_L^n} - \frac{k_p^2\sigma_z^2}{4}\right) \times \sin k_p\zeta. \tag{2.15}$$

Electrons are accelerated by the axial field (2.14) while executing betatron oscillations in the radial field (2.15) if they are in the accelerating and focusing phase of the wakefield, which occurs over a quarter period of each wake oscillation ($0 \leqslant k_p\zeta \leqslant \pi/2$).

3. Betatron oscillations and radiation damping in a super-Gaussian pulse-driven laser wakefield accelerator (LWFA)

3.1. Betatron oscillations

We focus on the transverse dynamics of electrons in wakefields. Because of the super-Gaussian nature we expect no harmonic betatron oscillations. Instead the betatron oscillations are non-harmonic and display very weak focusing force near the middle of the plasma channel and large restoring force only toward the edge of the wakefield. In super-Gaussian pulse-driven wakefields given by (2.14) and (2.15), for $r \ll r_L$, the focusing force can be approximately written as

$$F_r = -2n\frac{r^{n-1}}{r_L^n}\frac{\hat{E}_z}{E_0}\sin k_p\zeta, \tag{3.1}$$

where

$$\frac{\hat{E}_z}{E_0} = \frac{\sqrt{\pi}}{2} a_0^2 k_p \sigma_z \exp\left(-\frac{k_p^2\sigma_z^2}{4}\right). \tag{3.2}$$

The corresponding equation of betatron oscillation is

$$\frac{\mathrm{d}^2 x}{\mathrm{d}z^2} + \frac{K^2}{\gamma} x^{n-1} = 0, \tag{3.3}$$

where the focusing constant is calculated as

$$K^2 = \frac{2n}{r_L^n}\frac{\hat{E}_z}{E_0}\langle \sin k_p\zeta \rangle. \tag{3.4}$$

The envelope equation of the root-mean-square (rms) beam radius σ_{rb} is given by (Lee and Cooper, 1976; Swanekamp et al., 1992)

$$\frac{\mathrm{d}^2\sigma_{rb}}{\mathrm{d}z^2} + \frac{K^2}{\gamma}\sigma_{rb}^{n-1} - \frac{\varepsilon_{n0}^2}{\gamma^2\sigma_{rb}^3} = 0. \tag{3.5}$$

Assuming the beam energy γ as constant for now, this becomes

$$\frac{\mathrm{d}^2\sigma_{rb}^2}{\mathrm{d}z^2} + \kappa^2\sigma_{rb}^n = A, \tag{3.6}$$

where

$$\kappa^2 = \frac{2K^2}{\gamma}\frac{n+2}{n} = \frac{4(n+2)}{\gamma r_L^n}\frac{\hat{E}_z}{E_0}\langle \sin k_p\zeta \rangle, \tag{3.7}$$

and

$$A = 2\left(\frac{\mathrm{d}\sigma_{rb}}{\mathrm{d}z}\right)_{z=0}^2 + \frac{4K^2}{n\gamma}\sigma_{rb0}^n + \frac{2\varepsilon_{n0}^2}{\gamma^2\sigma_{rb0}^2}. \tag{3.8}$$

With $(\mathrm{d}\sigma_{rb}/\mathrm{d}z)_{z=0} = 0$, the equilibrium radius is obtained by setting $\mathrm{d}^2\sigma_{rb}^2/\mathrm{d}z^2 = 0$ as

$$\sigma_{rbM}^2 = \left(\frac{\varepsilon_{n0}}{K\sqrt{\gamma}}\right)^{4/(n+2)}. \tag{3.9}$$

3.2. Radiation damping

The synchrotron radiation causes the energy loss of beams and affects the energy spread and transverse emittance via the radiation reaction force (Jackson, 1999). The motion of an electron traveling along z-axis in the accelerating field E_z and the focusing force

https://doi.org/10.1017/S0022377812000311 Published online by Cambridge University Press

from the plasma wave evolves according to

$$\frac{\mathrm{d}u_x}{c\mathrm{d}t} = -K^2 x^{n-1} + \frac{F_x^{\mathrm{rad}}}{m_e c^2}, \tag{3.10}$$

$$\frac{\mathrm{d}u_z}{c\mathrm{d}t} = k_p \frac{E_z}{E_0} + \frac{F_z^{\mathrm{rad}}}{m_e c^2}, \tag{3.11}$$

where $\mathbf{F}^{\mathrm{rad}}$ is the radiation reaction force and $\mathbf{u} = \mathbf{p}/m_e c$ is the normalized electron momentum. The classical radiation reaction force is (Jackson, 1999)

$$\frac{\mathbf{F}^{\mathrm{rad}}}{m_e c \tau_R} = \frac{\mathrm{d}}{\mathrm{d}t}\left(\gamma \frac{\mathrm{d}\mathbf{u}}{\mathrm{d}t}\right) + \gamma \mathbf{u}\left[\left(\frac{\mathrm{d}\gamma}{\mathrm{d}t}\right)^2 - \left(\frac{\mathrm{d}\mathbf{u}}{\mathrm{d}t}\right)^2\right], \tag{3.12}$$

where $\gamma = (1+u^2)^{1/2}$ is the relativistic Lorentz factor of the electron and $\tau_R = 2r_e/3c \simeq 6.26 \times 10^{-24}$ s. Since the scale length of the radiation reaction $c\tau_R$ is much smaller than that of the betatron motion, assuming that the radiation reaction force is a perturbation and $u_z \gg u_x$, the equations of motion (3.10) and (3.11) are approximately written as

$$\frac{\mathrm{d}u_x}{\mathrm{d}t} \simeq -cK^2 x^{n-1} - c^2 \tau_R K^2 u_x (1 + K^2 \gamma x^{2(n-1)}), \tag{3.13}$$

$$\frac{\mathrm{d}u_z}{\mathrm{d}t} \simeq \omega_p \frac{E_z}{E_0} - c^2 \tau_R K^4 \gamma^2 x^{2(n-1)}, \tag{3.14}$$

$$\frac{\mathrm{d}x}{\mathrm{d}t} = \frac{cu_x}{\gamma} \simeq c\frac{u_x}{u_z}. \tag{3.15}$$

Finally, the particle dynamics are obtained from the following coupled differential equations:

$$\frac{\mathrm{d}^2 x}{\mathrm{d}t^2} + \left(\frac{\omega_p}{\gamma}\frac{E_z}{E_0} + \tau_R c^2 K^2\right)\frac{\mathrm{d}x}{\mathrm{d}t} + \frac{c^2 K^2}{\gamma} x^{n-1} = 0, \tag{3.16}$$

$$\frac{\mathrm{d}\gamma}{\mathrm{d}t} = \omega_p \frac{E_z}{E_0} - \tau_R c^2 K^4 \gamma^2 x^{2(n-1)}. \tag{3.17}$$

On the right-hand side of (3.17) the accelerating force (if it is in the accelerating phase) and the radiation damping term compete. If radiation damping is significant, electrons that were originally in the accelerating phase may fall into the decelerating phase and fall out of the rest of the bunch. However, in this current study we neglect this detrapping phenomenon and concentrate only on transverse dynamics. In (3.16) the last term is the super-Gaussian restoring force, while the second term makes the betatron oscillations to damp.

3.3. *Particle orbits in super-Gaussian wakefields*

In this section we investigate the behavior of a single particle which is accelerated in Gaussian/super-Gaussian wakefields, using the analysis described above. The particle orbit is obtained from the coupled differential equations describing the single particle dynamics (3.16) and (3.17). The equations are integrated numerically using the implicit Runge–Kutta algorithm. We want to compare the Gaussian wakefield case ($n = 2$) with different super-Gaussian cases ($n = 4, 6, 200$) qualitatively. Figure 1 shows the particle orbits for a single particle in Gaussian and different super-Gaussian cases. In the Gaussian wakefield, as we know (Michel et al., 2006; Nakajima et al., 2011), electrons execute rapid betatron oscillations and synchrotron radiation makes these oscillations damp. In $n = 4$, non-harmonic betatron oscillations occur, whose periods get longer as the electron gains energy. The initial transverse velocity of the particle was set to zero, while it was displaced 10^{-5} m in transverse direction with respect to the laser beam axis. We assume a constant accelerating gradient in z-direction of $E_z = 1.5\,\mathrm{GVm}^{-1}$. The plasma density is $n_e = 10^{15}$ cm^{-3} (see Nakajima et al., 2011). In this parameter regime, electrons may be accelerated toward 0.5 TeV over a single stage. The visible tendency is that toward a higher order of n, the particle oscillates less. In our example, for $n \geqslant 6$, the trajectory eventually gets ballistic. In these cases (n large) most of the electrons with small x remain in that region and execute straight orbit till the end of the accelerator. This property is helpful to maintain the initial small emittance. We note that the order of n from which the trajectory of the particle gets ballistic depends on initial parameters of the particle as well as on the parameters of the experimental setup. However, the general trend is valid for any kind of initial parameters and confirms our expectation. In the higher order super-Gaussian cases a small initial transverse velocity tends to stay small. This also indicates a smaller increase of transverse momentum spread during acceleration when using higher order super-Gaussian powers and, therefore, a smaller increase of emittance.

4. Discussion and conclusion

We have introduced an analytical treatment for laser wakefields induced by super-Gaussian laser pulses in the quasi-linear regime. The super-Gaussian laser pulse may be able to excite the laser wakefield whose transverse fields are much weaker than that driven by a Gaussian laser. This helps to reduce the betatron oscillations and allows us to inject electron beams with smaller emittance even with a large diameter of the aperture of plasma. This allows for a greater number of beam particles while keeping the emittance small.

An equation for the matched beam radius with dependence on the super-Gaussian power n is derived. An example of the dependence (3.9) is shown in Fig. 2 for an initial emittance of 10 μm and an initial γ of 2000 with a plasma density of 10^{15} cm^{-3}. It shows an increase of the matched beam radius toward increasing n while leaving the initial value for the emittance and γ constant. Since the maximum loaded charge in the beam $Q_b \sim \sigma_{x0}^2$ and, therefore the maximum particle number in the beam $N_b \sim \sigma_{x0}^2$, a larger matched beam radius allows for a larger number of particles per bunch, leaving the initial emittance constant and preferably small. For collider application, both a small emittance and a large number of particles per bunch are essential, since both variables enter the equation for geometric luminosity

https://doi.org/10.1017/S0022377812000311 Published online by Cambridge University Press

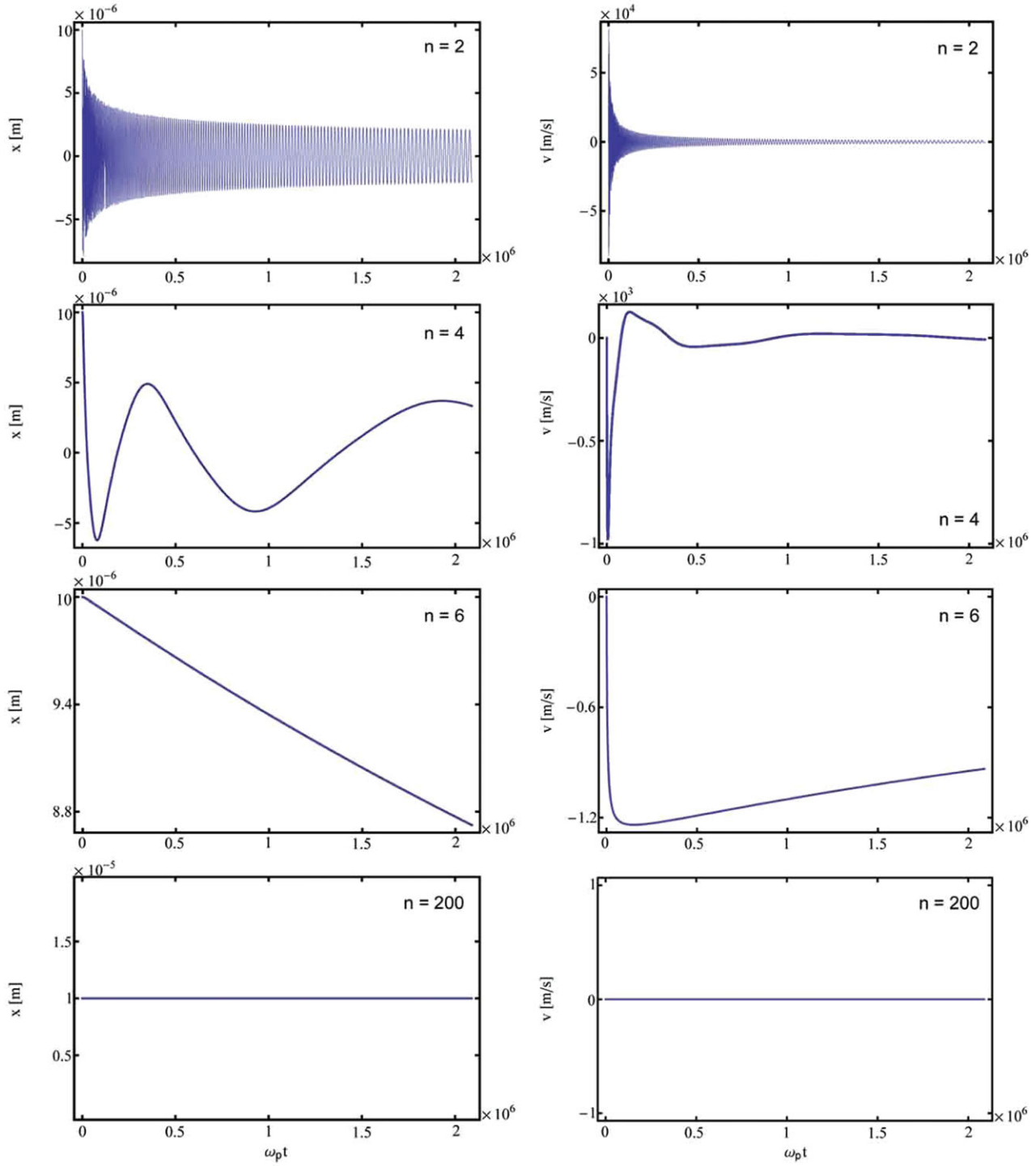

Figure 1. (Colour online) Transverse position and transverse velocity of a single particle accelerated in Gaussian/super-Gaussian laser wakefields. The initial offset of the particle with respect to the laser beam axis is 10^{-5} m, the initial transverse velocity is zero. The accelerating gradient, $E_z = 1.5$ GVm^{-1}, and the plasma density is $n_e = 10^{15}$ cm^{-3}. The final value of $\omega_p t$ corresponds to a stage length of 333 m and the final energy $\gamma_f = 10^6$.

(e.g. Edwards and Edwards, 2008),

$$\mathscr{L} = \frac{N_b^2 f_c}{4\pi\sigma_x\sigma_y} = \gamma\frac{N_b^2 f_c}{4\pi\varepsilon_n\beta^*}, \tag{4.1}$$

where f_c is the collision frequency, ε_n is the transverse normalized emittance, and β^* is the betatron function at collision point. Furthermore, σ_x and σ_y are the transverse rms beam sizes at collision point and $\sigma_x \sim \sigma_y \sim \sqrt{\beta^*\varepsilon_n/\gamma}$, assuming a round beam.

While the super-Gaussian approach seems promising, there are limitations on the applicability of this approach, which we estimate in the following. For a low-density LWFA ($n_e = 10^{-15}$ cm^{-3}) a long propagation distance is important to reach high particle energies (333 m in our example). The super-Gaussian pulse limits

https://doi.org/10.1017/S0022377812000311 Published online by Cambridge University Press

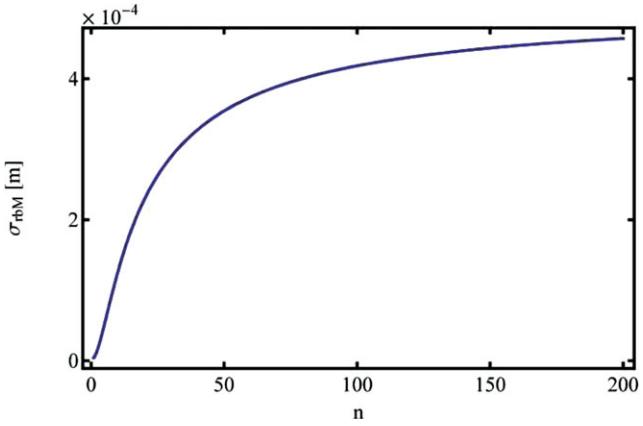

Figure 2. (Colour online) Matched beam radius σ_{rbM} for an emittance $\varepsilon_{nx} = 10\,\mu$m and $\gamma = 2000$ with a plasma density $n_e = 10^{15}$ cm^{-3} and a laser spot size $r_L = 504$ μm versus the super-Gaussian power n.

the acceleration distance because of the deformation of its pulse shape, which occurs due to different group velocities of the fundamental Gaussian mode and the higher order super-Gaussian modes when pulse propagates in a plasma channel. For a matched laser case, the group velocity of the Laguerre–Gaussian mode propagating in a parabolic density channel is given by (Schroeder et al., 2011)

$$\beta_g = \frac{v_g}{c} = 1 - \frac{k_p^2}{2k_0^2} - \frac{2(1+N)}{k_0^2 r_L^2}, \tag{4.2}$$

where v_g is the laser group velocity, $k_0 = \omega_0/c = 2\pi/\lambda_0$ is the laser wave number with laser frequency ω_0 and the laser wavelength λ_0, r_L is the laser spot radius, and $N = n - 2$ in our estimation. This means that the group velocity of the higher order modes is slower than fundamental Gaussian mode ($N = 0$). Assuming that the super-Gaussian mode is composed by superposition of the higher order modes up to the mode number N, a characteristic length of pulse lengthening because of higher order mode slippage is estimated to be

$$L_{\text{slippage}} \approx c\tau_L \left(\frac{1}{\beta_{gN}} - \frac{1}{\beta_{g0}}\right)^{-1} \approx \frac{c\tau_L k_0^2 r_L^2}{2N} \times \left(1 - \frac{k_p^2}{k_0^2} - \frac{2(2+N)}{k_0^2 r_L^2}\right), \tag{4.3}$$

where $c\tau_L$ is the initial pulse length. For the low-density plasma with $k_p^2/k_0^2 = n_e/n_c \ll 1$, the mode slippage length is

$$L_{\text{slippage}} \approx \frac{c\tau_L k_0^2 r_L^2}{2N} = \frac{c\tau_L k_p^2 r_L^2}{2N}\frac{n_c}{n_e}, \tag{4.4}$$

where $n_c = \pi/(r_e\lambda_0^2)$ is the critical plasma density with the classical electron radius r_e. In our numerical example, setting $k_p r_L = 3$ and $k_p\sigma_L = 1$ with the rms pulse length $\sigma_L = c\tau_L/2\sqrt{\ln 2}$, the mode slippage is approximately given by

$$L_{\text{slippage}} \approx \frac{9\sqrt{\ln 2}\lambda_0}{2\pi(n-2)}\left(\frac{n_c}{n_e}\right)^{3/2} \approx \frac{2.1\text{ km}}{(n-2)}\left(\frac{1\,\mu\text{m}}{\lambda_0}\right)^2 \times \left(\frac{10^{15}\text{ cm}^{-3}}{n_e}\right)^{3/2}, \tag{4.5}$$

where $n = N + 2$ is the mode number of the super-Gaussian mode. In the numerical example, the stage length, $L_{\text{stage}} = 333$ m, is shorter than the slippage length, $L_{\text{slippage}} = 350$ m, for the super-Gaussian mode $n = 8$. Therefore, the allowable maximum mode number of the super-Gaussian mode for the stage length of 333 m at the plasma density $n_e = 10^{15}$ cm^{-3} is $n \leqslant 8$. For higher order super-Gaussian modes, the slippage distance becomes shorter than the required acceleration distance. For example, with $n = 200$ and $n_e = 10^{15}$ cm^{-3} the slippage distance becomes $L_{\text{slippage}} \approx 11$ m.

However, the pulse lengthening effect may be compensated by pulse etching (Lu et al., 2007) and/or pulse self-compression that occurs in conjunction with the group velocity dispersion (GVD) of plasma (Faure et al., 2005). In fact the multi-dimensional particle-in-cell (PIC) simulations show that the front of the laser pulse exciting the wake moves backward due to local pump depletion at the etching rate, $v_{\text{etch}} \approx c\omega_p^2/\omega_0^2 = cn_e/n_c$. Consequently, the pulse lengthening rate may be significantly reduced as $v_{\text{slippage}} - v_{\text{compression}}$, where $v_{\text{slippage}} \approx v_{g0} - v_{gN} \approx c(2N/k_p^2 r_L^2)(n_e/n_c)$ is the mode slippage rate and $v_{\text{compression}} \approx v_{\text{etch}} + v_{\text{self-comp}}$ is the pulse compression rate. With $v_{\text{compression}} \approx \alpha_{\text{comp}} cn_e/n_c$, one may find the optimum mode number of the super-Gaussian pulse as

$$n \approx \frac{\alpha_{\text{comp}}}{2} k_p^2 r_L^2 + 2, \tag{4.6}$$

for which the pulse length of the super-Gaussian pulse remains constant over acceleration distance.

Until here the discussion in this paper is focused only to the low-density linear or quasi-linear regime. For LWFA regimes other than that, i.e. the nonlinear bubble or blowout regime (Kostyukov et al., 2004; Lu et al., 2006) we are pessimistic that the super-Gaussian approach (or other modified pulse shapes) could help to improve the performance of such accelerators. This is because, as described in Sec. 2, the flat-top-tailored transverse profile of the super-Gaussian laser ponderomotive potential is imprinted on the transverse distribution of the wake potential only in conjunction with the linear plasma response. Furthermore, the focusing force in the nonlinear regime is larger than that in the linear wakefields driven by Gaussian and super-Gaussian pulses given by (3.1). Strong focusing force on electrons (defocusing force on positrons) in the nonlinear bubble regime is harmful for the desired collider applications that require extremely high-quality electron and positron beams with small longitudinal and transverse emittances as well as easy production of mono-energetic beams.

https://doi.org/10.1017/S0022377812000311 Published online by Cambridge University Press

For the collider application, the operation in low-density linear or quasi-linear regime, as described by Nakajima et al. (2011), has many advantages. In this regime the super-Gaussian pulse-driven LWFA might help to improve the beam quality as discussed in this paper. While efforts to tailor the focusing forces in the quasi-linear LWFA regime exist (Cormier-Michel et al., 2009; Geddes et al., 2010), there is more theoretical as well as experimental research needed in future to gain more insight.

Acknowledgements

The work has been supported by the Munich Centre for Advanced Photonics, the National Natural Science Foundation of China (Project Nos. 10834008, 60921004 and 51175324), and the 973 Program (Project No. 2011CB808104). K. Nakajima is supported by Chinese Academy of Sciences Visiting Professorship for Senior International Scientists (Grant No. 2010T2G02).

References

Brozek-Pluskab, B., Gliger, D., Hallou, A., Malka, V. and Gauduel, Y. A. 2005 *Radiat. Phys. Chem.* **72**, 149.

Cheshkov, S., Tajima, T., Horton, W. and Yokoya, K. 2000 *Phys. Rev. ST Accel. Beams* **3**, 071301.

Chiu, C., Cheshkov, S. and Tajima, T. 2000 *Phys. Rev. ST Accel. Beams* **3**, 101301.

Clayton, C. E. et al. 2010 *Phys. Rev. Lett.* **105**, 105003.

Cormier-Michel, E., Esarey, E., Geddes, C. G. R., Schroeder, C. B. and Leemans, W. P. 2009 *Proceedings of ICAP '09* pp. 281–284.

Crowell, R., Gosztola, D. J., Shkrob, I. A., Oulianov, D. A., Jonah, C. D. and Rajh, T. 2004 *Radiat. Phys. Chem.* **70**, 501.

Edwards, D. A. and Edwards, H. T. 2008 *Reviews of Accelerator Science and Technology*, Vol. 1. Singapore: World Scientific.

Faure, J., Glinec, Y., Pukhov, A., Kiselev, S., Gordienko, S., Lefebvre, E., Rousseau, J.-P., Burgy, F. and Malka, V. 2004 *Nature* **431**, 541.

Faure, J., Glinec, Y., Santos, J. J., Ewald, F, Rousseau, J.-P., Kiselev, S., Pukhov, A., Hosokai, T. and Malka, V. 2005 *Phys. Rev. Lett.* **95**, 205003.

Faure, J., Rechatin, C., Norlin, A., Lifschitz, A., Glinec, Y. and Malka, V. 2006 *Nature* **444**, 737.

Froula, D. H. et al. 2009 *Phys. Rev. Lett.* **103**, 215006.

Geddes, C. G. R., Cormier-Michel, E., Esarey, E., Schroeder, C. B. and Mullowney, P. 2010 *AIP Conf. Proc.* **1299**, 197.

Geddess, C. G. R., Toth, C., van Tilborg, J., Esarey, E., Schroeder, C. B., Bruhwiler, D., Nieter, C., Cary, J. and Leemans, W. P. 2004 *Nature* **431**, 538.

Giulietti, A. et al. 2008 *Phys. Rev. Lett.* **101**, 105002.

Gorbunov, L. M. and Kirsanov, V. I. 1987 *Sov. Phys. JETP* **66**, 290.

Hafz, N. A. M. et al. 2008 *Nature Photonics* **2**, 571.

Hamster, H., Sullivan, A., Gordon, S., White, W. and Falcone, R. W. 1993 *Phys. Rev. Lett.* **71**, 2725.

Jackson, J. D. 1999 *Classical Electrodynamics*, 3rd edn. New York: Wiley.

Kameshima, T. et al. 2008 *Appl. Phys. Express* **1**, 066001.

Karsch, S. et al. 2007 *New J. Phys.* **9**, 415.

Kostyukov, I., Pukov, A. and Kiselev, S. 2004 *Phys. Plasmas* **11**, 5256.

Lee, E. P. and Cooper, R. K. 1976 *Part. Accel.* **7**, 83.

Leemans, W. P., Nagler, B., Gonsalves, A. J., Toth, C., Nakamura, K., Geddes, C. G. R., Esarey, E., Schroeder, C. B. and Hooker, S. M. 2006 *Nature Phys.* **2**, 696.

Leemans, W. P. et al. 2003 *Phys. Rev. Lett.* **91**, 074802.

Liu, J. S. et al. 2011 *Phys. Rev. Lett.* **107**, 035001.

Lu, W., Huang, C., Zhou, M., Mori, W. B. and Katsouleas, T. 2006 *Phys. Rev. Lett.* **96**, 165002.

Lu, W., Tzoufras, M., Joshi, C., Tsung, F. S., Mori, W. B., Vieira, J., Fonseca, R. A. and Silva, L. O. 2007 *Phys. Rev. ST Accel. Beams* **10**, 061301.

Lundh, O. et al. 2011 *Nature Phys.* **7**, 219.

Mangles, S. P. D. et al. 2004 *Nature* **431**, 535.

McGuffey, C. et al. 2010 *Phys. Rev. Lett.* **104**, 025004.

Michel, P., Schroeder, C. B., Shadwick, B. A., Esarey, E. and Leemans, W. P. 2006 *Phy. Rev. E* **74**, 026501.

Modena, A. et al. 1995 *Nature* **337**, 606.

Nakajima, K. et al. 1995 *Phys. Rev. Lett.* **74**, 4428.

Nakajima, K. et al. 2011 *Phys. Rev. ST Accel. Beams* **14**, 091301.

Osterhoff, J. et al. 2008 *Phys. Rev. Lett.* **101**, 085002.

Pak, A., Marsh, K. A., Martins, S. F., Lu, W., Mori, W. B. and Joshi, C. 2010 *Phys. Rev. Lett.* **104**, 025003.

Pollock, B. B. et al. 2011 *Phys. Rev. Lett.* **107**, 045001.

Schmid, K., Buck, A., Sears, C. M. S., Mikhailova, J. M., Tautz, R., Herrmann, D., Geissler, M., Krausz, F. and Veisz, L. 2010 *Phys. Rev. ST Accel. Beams* **13**, 091301.

Schroeder, C. B., Benedetti, C., Esarey, E., van Tilborg, J. and Leemans, W. P. 2011 *Phys. Plasmas* **18**, 083103.

Schroeder, C. B., Esarey, E., Geddes, C. G. R., Benedetti, C. and Leemans, W. P. 2010 *Phys. Rev. ST Accel. Beams* **13**, 101301.

Sprangle, P., Esarey, E., A. Ting, and G. Joyce 1988 *Appl. Phys. Lett.* **53**, 2146.

Swanekamp, S. B., Holloway, J. P., Kammash, T. and Gilgenbach, R. M. 1992 *Phys. Fluids* B **4**, 1332.

Tajima, T. 1985 *Laser Part. Accel.* **3**, 351.

Tajima, T. and Dawson, J. M. 1979 *Phys. Rev. Lett.* **43**, 267.

van Outheusden, T., Pasmans, P. L. E. M., van der Geer, S. B., de Loos, M. J., van der Wiel, M. J. and Luiten, O. J. 2010 *Phys. Rev. Lett.* **105**, 264801.

Xie, M., Tajima, T., Yokoya, K. and Chattopadyay, S. 1997 *AIP Proc.* **398**, 232.